Research Article | Vol. 26, No. 26 | 24 Dec 2018 | OPTICS EXPRESS 34699

Optics EXPRESS

Beat frequency tuning in dual-polarization distributed feedback fiber laser using side polishing technique

KUIKUI GUO,[1] JUN HE,[1,*] SHAOQING CAO,[1] MAOXIANG HOU,[1] ZHE ZHANG,[1] GAIXIA XU,[1] AND YIPING WANG[1,2]

[1]*Key Laboratory of Optoelectronic Devices and Systems of Ministry of Education and Guangdong Province, College of Optoelectronic Engineering, Shenzhen University, Shenzhen 518060, China*
[2]*ypwang@szu.edu.cn*
[*]*hejun07@szu.edu.cn*

Abstract: We propose and demonstrate a method for tuning the beat frequency of a dual-polarization distributed feedback (DFB) fiber laser via fiber side polishing. This process can significantly alter the birefringence in DFB fiber lasers. Beat frequency evolutions in DFB fiber lasers were investigated, and the experimental results showed that the beat frequency tuning was dependent on polished thickness, roughness, and direction. The abrasive paper with a grain size of 1.8 μm was adopted to fine-tune the beat frequency. It was found that the beat frequency of DFB fiber lasers shifted toward higher frequencies with increasing polished thickness. However, the beat frequency shifted toward lower frequencies using a secondary side polishing process in the direction orthogonal to the first polished surface. As a result, the beat frequency of the DFB fiber laser was tuned in a wide frequency range from 475.5 MHz to 2080.4 MHz, which corresponds to a birefringence change of 1.2×10^{-5}. Side-polished DFB fiber lasers could provide a novel approach to frequency division multiplexing for a large number of fiber laser sensors.

1. Introduction

Distributed feedback (DFB) fiber lasers have the advantages of compact structure, high signal-to-noise ratio (SNR), and the capability of operating without longitudinal mode hoping [1–3]. These properties have attracted much attention in recent years as the DFB fiber lasers exhibit nearly ideal characteristics for applications in telecommunication systems [4,5], high-resolution spectroscopy and interferometry [6,7], microwave signal generation [8], high-performance sensor systems for measuring temperature [9], transverse pressure [10], acoustic signal [11], and gravitational wave [12], etc. These DFB fiber lasers were fabricated by optically pumping an active cavity consisting of a phase-shifted fiber Bragg grating (PS-FBG) directly inscribed on a rare-earth-doped fiber. Both intrinsic birefringence and UV-induced birefringence exist in the rare-earth-doped fiber. The intrinsic birefringence was introduced by geometrical imperfections in the fiber core and residual thermal stress at the core-cladding interface during fiber drawing process, whereas the UV-induced birefringence was generated by the unidirectional and asymmetric UV laser exposure in case the PS-FBG was fabricated [13,14]. The UV-induced birefringence and the intrinsic birefringence in the DFB fiber laser can produce a stable low beat frequency ranging from tens to hundreds of MHz [15]. This restricts their practical use in frequency division multiplexing (FDM) for multiple fiber laser sensors [16], in which a mixer and a local oscillator are always required to convert the beat frequency. In addition, this also limits the fabrication of single polarization DFB fiber lasers, yet the development of single polarization DFB fiber lasers is of great interest due to their wide range of applications [17]. Therefore, a new design approach for controlling DFB fiber laser birefringence is the focus of many researchers all the time.

#341460 https://doi.org/10.1364/OE.26.034699
Journal © 2018 Received 15 Aug 2018; revised 31 Oct 2018; accepted 31 Oct 2018; published 21 Dec 2018

Optics EXPRESS

A variety of approaches have been reported for altering the birefringence in optical fibers, such as by applying UV laser exposure [14–16,18], CO_2 laser exposure [19], femtosecond laser exposure [20], lateral stress [21], bend [22], twist [23,24], and side polishing [25], etc. In 1994, Vengsarkar *et al* first reported the reduction in fiber birefringence by ~1.5×10^{-5} using a UV laser dual-exposure technique [14]. Subsequently, this technique was developed for beat frequency tuning of dual-polarization fiber laser sensors. For example, Guo *et al* converted the low beat frequency of a distributed Bragg reflector (DBR) fiber laser at 18.6 MHz into a higher value of 131.6 MHz by applying UV laser irradiation on the laser cavity [15]. Zhang *et al* achieved a beat frequency tuning range of ~700 MHz and a birefringence change of ~5.1×10^{-6} in DBR fiber lasers using the same method [16]. Moreover, the CO_2 laser exposure was also used to alter the fiber birefringence. Using this method, Jin *et al* tuned the beat frequency from ~200 MHz to ~1.7 GHz, which corresponds to a birefringence change of ~1.2×10^{-5} [19]. They further implemented a 16-element multiplexed heterodyning DBR fiber laser sensors array by precisely adjusting the birefringence in each fiber laser cavity via CO_2 laser side irradiation [19]. In addition to these laser exposure methods, the mechanical methods, such as applying lateral stress, bend, and twist, were also reported for introducing extra birefringence. The typical values of the birefringence induced by lateral stress, bend, and twist are 1.0×10^{-5}, 4.8×10^{-5}, and 2.9×10^{-6}, respectively [21–23]. Nevertheless, the birefringence created by these mechanical methods relies on the external forces applied on the fiber. Hence, these methods could not provide a stable, permanent, and repeatable technique for tuning the beat frequency of fiber lasers.

The side polishing on optical fiber was also used to alter the birefringence. In 1986, Stolen showed that polishing the fiber could introduce a birefringence change, which first rose to a maximum and then felled off as the polished surface approached the core [25]. As a result, a polishing-induced-birefringence of up to 9.0×10^{-5} in single-mode fiber (SMF) was achieved experimentally. Additionally, we previously reported on an on-line fiber side polishing method using a motor-driven polishing wheel together with a broadband light source and an optical spectrometer [26,27]. The polished thickness of the fibers could be precisely controlled using this method, and this will be beneficial for precisely altering the fiber birefringence. As a result, it is possible to obtain a novel, stable, and convenient technique for fine-tuning the beat frequency of dual-polarization fiber lasers with the side polishing method.

In this paper, we demonstrated a novel method for tuning the beat frequency of DFB fiber lasers via fiber side polishing. This method can alter the birefringence in the DFB fiber laser cavity. The beat frequency evolutions of DFB fiber lasers were studied with varying polished thickness, roughness, and direction. We found that the beat frequency tuning was dependent on polished thickness, roughness, and direction. Beat frequency of the DFB fiber laser shifted toward higher frequencies with increasing polishing thickness. Moreover, the beat frequency shifted toward lower frequencies with a secondary side polishing process in the direction vertical to the first fiber polished surface, and the beat frequency of the DFB fiber laser was tuned in a wide frequency range from 475.5 MHz to 2080.4 MHz. Therefore, this process can provide a novel approach for multiplexing a large number of fiber laser sensors, and also can provide a promising technique for fabricating single polarization DFB fiber lasers.

2. Principle of operation

The structure of a side-polished DFB fiber laser and the schematic diagram of beat frequency measurement system are shown in Fig. 1. The resonant cavity of the side-polished DFB fiber laser consists of a side-polished PS-FBG, which was first directly inscribed on a short section of erbium doped optical fiber (EDF) and then polished from the fiber surface on one side. The output from a pump laser diode (LD) operating at the wavelength of 980 nm was launched into the fiber laser cavity (i.e. the PS-FBG on EDF) through a wavelength division multiplexer (WDM), and a SMF (Corning SMF-28) with a core/cladding diameter of 8.2/125 μm was spliced with the EDF. The backward emitting DFB fiber laser output was directed into a high speed photodetector (PD, Newfocus 1592) through an isolator (ISO, Golight ISO-1550-S), which was used to isolate the emitting laser that reflected from the fiber end face. Due to the unique structure of laser cavities, these DFB fiber lasers can operate in a reliable and stable single longitudinal mode without mode hopping [28]. Nevertheless, two orthogonal polarization modes, denoted as x and y polarization, exist in the DFB fiber laser due to the UV-induced birefringence and intrinsic fiber birefringence [29]. The beat signal was generated by the two polarization modes and monitored with a radio frequency (RF) spectrum analyzer (Rohde & Schwarz FSV4).

The laser cavity (i.e. the PS-FBG on EDF) of the DFB fiber laser was side polished with a designed polished thickness in the selected polishing direction. Hence, the birefringence in the side-polished DFB fiber laser could be precisely determined due to the introduction of the asymmetric structure and anisotropic stress distribution. According to the previous studies [25], the side-polishing-induced birefringence is dependent on the polished thickness. As a result, the beat frequency of the DFB fiber laser could be fine-tuned by carefully adjusting the side polishing parameters, such as polished thickness (0.7 – 8.0 μm), roughness (3000, 5000, and 7000 mesh), and direction ($\theta = 0°$, + 45°, and + 90°).

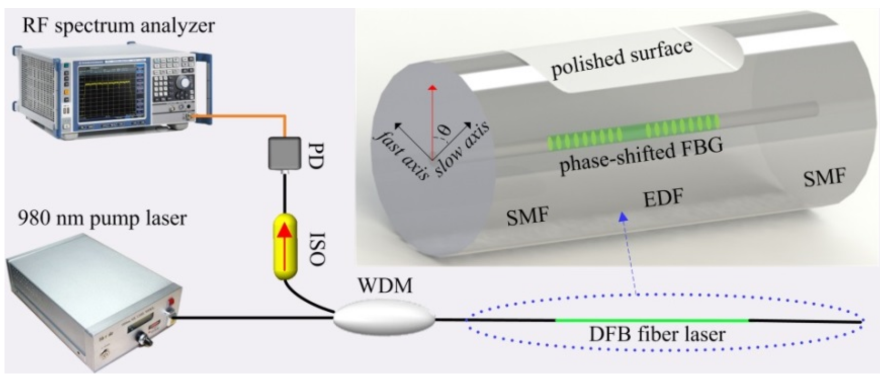

Fig. 1. The structure of a side-polished distributed feedback (DFB) fiber laser and schematic diagram of beat frequency measurement system.

The original fast and slow axes in the DFB fiber laser cavity should be found out before side polishing. The direction with a higher refractive index n_x is defined as the slow axis x, whereas the orthogonal direction with a lower refractive index n_y is defined as the fast axis y. The slow and fast axes can be distinguished by examining the transverse-load response of the DFB fiber laser to various loading orientations. This is similar to the process described in [30], in which a positive maximum frequency shift (i.e. toward higher frequencies) occurs along fast axis, whereas a negative maximum shift occurs (i.e. toward lower frequencies) along slow axis. The angle between the vector normal to the polished surface and the original slow axis was defined as θ, as illustrated in Fig. 1.

The wavelengths of the two polarization modes are given by Guan *et al* [28]:

$$\lambda_x = 2n_x\Lambda, \lambda_y = 2n_y\Lambda, \tag{1}$$

where n_x and n_y are the effective refractive indices of the two orthogonal polarization modes, and Λ is the fiber grating period. Hence, the separation between the two orthogonal emitting wavelengths in the DFB fiber laser can be expressed as:

$$\Delta\lambda = \lambda_x - \lambda_y = 2B\Lambda, \tag{2}$$

where the $B = n_x\text{-}n_y$ is the fiber birefringence. The DFB fiber laser output was monitored with a high speed PD and RF spectrum analyzer, as shown in Fig. 1. The fiber laser produces a beat signal at the beat frequency given by [28]:

$$\Delta\nu = v_x - v_y = \frac{c}{\lambda_x} - \frac{c}{\lambda_y} = \frac{cB}{n_0\lambda_0}. \tag{3}$$

where $n_0 = (n_x + n_y)/2 \approx n_x \approx n_y$ is the average refractive index of the fiber grating, c is the speed of light in vacuum, and λ_0 is the emitting wavelength of the DFB fiber laser. Equation (3) suggests the variations in the birefringence B can lead to the shifts in the beat frequency. By differentiating Eq. (3), the birefringence variations δB can be expressed as:

$$\delta B = \frac{\delta\Delta\nu \cdot n_0\lambda_0}{c} = \frac{\delta\Delta\nu \cdot \lambda_0^2}{2c\Lambda}. \tag{4}$$

Based on this theoretical analysis, we can induce changes in the birefringence B using the side polishing method to produce an asymmetric structure. From Eq. (4), we can calculate the birefringence variation δB of a DFB fiber laser from the parameter $\delta\Delta\nu$ (i.e. beat frequency shift).

3. Experimental setup

The original DFB fiber laser was fabricated before side polishing and is shown in the inset of Fig. 2. A π PS-FBG with a total length of 46 mm, a shielded phase-shifted section length of ~1.5 mm, and a central wavelength of 1549.94 nm was inscribed on a 65 mm-long highly Er^{3+}-doped fiber (EDF, Nufern SM-ESF-7/125, peak absorption: 55 dB/m @ 1530 nm) using a scanning UV laser beam with a shielded phase mask. This fabrication method is similar to that of our previous study [31]. The EDF was loaded with hydrogen (80 °C and 13 MPa for 7 days) to increase the fiber photosensitivity. Subsequently, the EDF was spliced with two SMFs, and the splicing loss was ~0.2 dB. After the π PS-FBG was successfully fabricated on the EDF, a 980 nm pump laser was launched into the DFB fiber laser cavity (i.e. the PS-FBG on EDF). The DFB fiber laser generated a backward emitting output at a lasing wavelength of 1549.94 nm. Figure 2 demonstrates the output power of the DFB fiber laser versus the input pump power. The DFB fiber laser exhibits a threshold pump power of 14.9 mW and a slope efficiency of 0.43%.

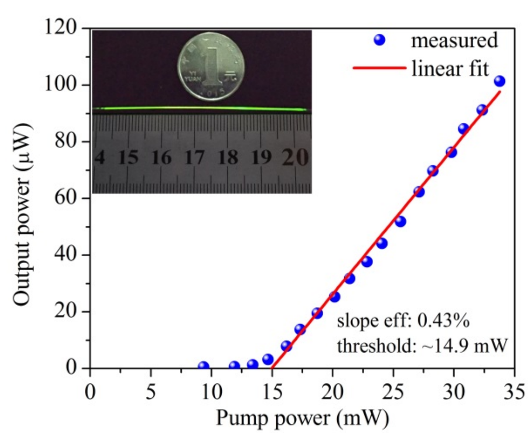

Fig. 2. The output power of the DFB fiber laser as a function of 980 nm laser pump power. (inset: the original DFB fiber laser before side polishing;)

Figure 3 shows the experimental setup used for DFB fiber laser side polishing. A motor-driven wheel polishing system (WanRun Ltd.) was employed in the experimental setup. A cylindrical grinding wheel was mounted on a precise 3-dimension translation platform which could be moved in the X, Y and Z directions via computer controls. The entire π PS-FBG on the EDF was side polished by a designed thickness. At first, the two SMFs connecting the two ends of the DFB fiber laser were fixed by a pair of fiber holders in a selected direction (i.e. at an angle θ with the original slow axis, which was found out from the transverse-load response of the DFB fiber laser [30]). A weight was hung on one end to maintain constant tension in the fiber. Subsequently, a 62 mm diameter polishing wheel lined with an abrasive paper (STABCKE, Warriors 991A, Germany), as shown in the inset of Fig. 3, was lowered by presetting the height of the wheel in the Z direction to ensure a close contact of the abrasive paper with the EDF. And then, the polishing wheel was translated across the DFB fiber laser in the Y direction. The rolling speed of the wheel and the distance traveled in the Y direction were preset using a personal computer (PC). The EDF containing the π PS-FBG was gradually polished by a back-and-forth motion of the rolling wheel along the fiber. During the fiber side polishing process, both the optical spectrum and the RF frequency spectrum of the DFB fiber laser were monitored. The backward emitting laser output was launched into a 3 dB coupler through an isolator. The output laser was divided into two branches. One branch was detected by an optical spectrum analyzer (OSA, YOKOGAWA AQ6370C) with a resolution of 0.02 nm. The DFB fiber laser spectra could then be monitored. The other branch was projected into a high speed PD and the beat signal from the DFB fiber laser was monitored using an RF spectrum analyzer with a resolution bandwidth (RBW) set to be 10 kHz.

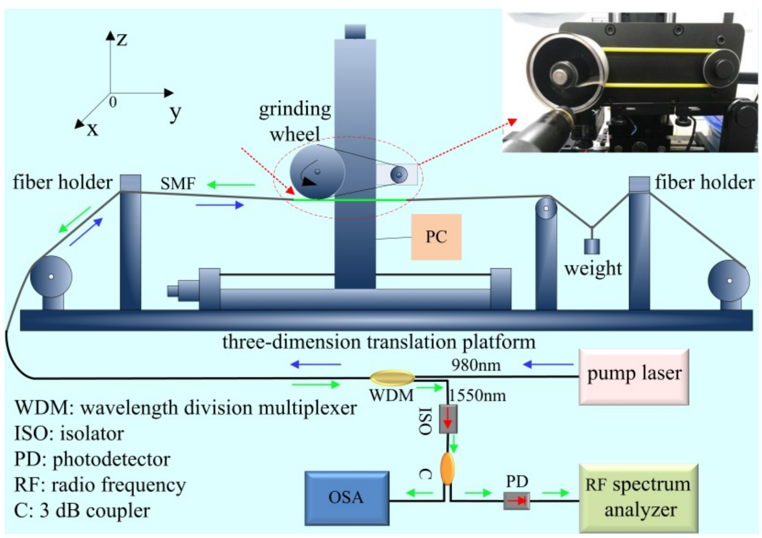

Fig. 3. The experimental setup including a motor-driven wheel polishing system employed for DFB fiber laser side polishing (inset: a 62 mm diameter polishing wheel lined with an abrasive paper).

4. Results and discussion

A DFB fiber laser was side polished by a thickness of 1.3 μm with a 7000 mesh abrasive paper in the direction at an angle $\theta = +\ 45°$ with the original slow axis. Figure 4 shows the beat signals and optical spectra of the DFB fiber laser before and after side polishing. The pump power was fixed to 130 mW in this experiment. As shown in Figs. 4(a) and 4(c), the beat frequency shifted rapidly toward higher frequencies from initial 152.4 MHz to 1014.5 MHz. The corresponding birefringence variation δB was 6.5×10^{-6}. The signal-to-noise ratio (SNR) of the beat signal decreased slightly from 43.4 dB to 40.8 dB. Nevertheless, the lasing wavelength of the DFB fiber laser remained mostly unchanged (i.e. 1549.94 nm), as shown in

Figs. 4(b) and 4(d). The SNR in the optical spectrum also decreased slightly from 39.4 dB to 36.8 dB. These results indicate that the birefringence in EDFs could be noticeably altered using the side polishing method, and hence the beat frequency of the DFB fiber laser could be tuned via fiber side polishing.

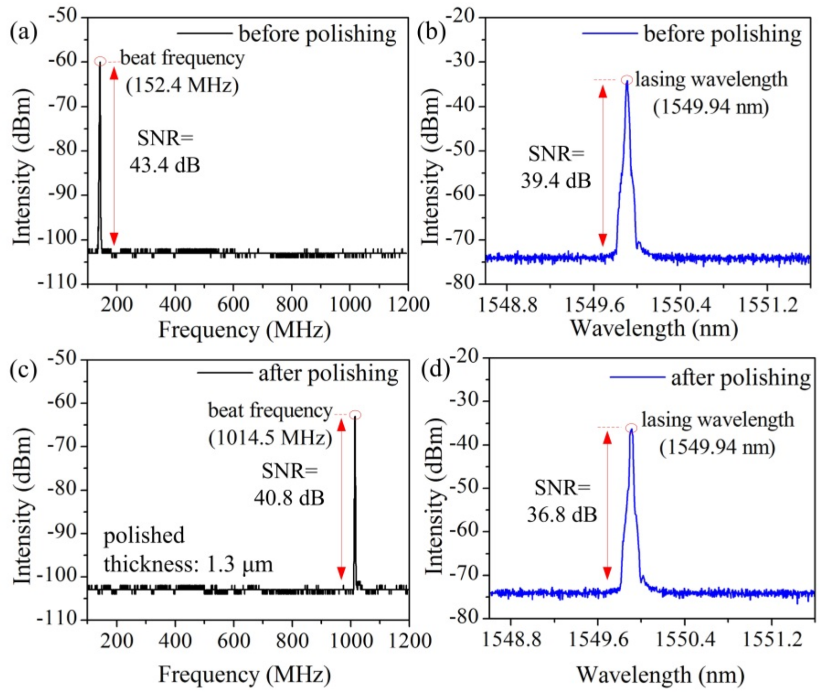

Fig. 4. Beat signal (a) and optical spectrum (b) of the DFB fiber laser before side polishing, and beat signal (c) and optical spectrum (d) of the DFB fiber laser after side polishing.

An additional test was conducted to verify that the beat frequency shift in the previous polishing experiment was irrelevant to the axial strain on EDF. Various weights were hung on the SMF connected to one end of the DFB fiber laser, as shown in Fig. 3. The beat signals and optical spectra of the DFB fiber laser under various weights are shown in Figs. 5(a) and 5(c), respectively. The beat frequency and lasing wavelength are extracted and then demonstrated in Figs. 5(b) and 5(d), respectively. It is obvious that the applied axial strain could hardly change the beat frequency, which exhibits an extremely low sensitivity of ~-3 × 10^{-4} MHz/g to the weights and a maximum frequency shift of less than 0.05 MHz. This could be explained by the fact that the axial strain applied on an EDF generates the same refractive index change in the fast and slow axes (i.e. $\delta n_x = \delta n_y$), and hence could hardly change the fiber birefringence. However, the lasing wavelength of the same DFB fiber laser shifted toward longer wavelengths with increasing weights, resulting from the strain-induced refractive index changes through photo-elastic effect and the variations in the PS-FBG pitches. The sensitivity of the lasing wavelength to the hung weights is 5.6 pm/g. It means the axial strain applied on the DFB fiber laser can only induce a lasing wavelength shift but has a negligible effect on the beat frequency. Therefore, the beat frequency shift in the side polishing process should be introduced by the change in fiber geometry or stress distribution instead of the axial strain applied during side polishing. Moreover, the results also demonstrate that this type of DFB fiber lasers may further be used for dual-parameter sensing by simultaneously detecting the beat frequency and lasing wavelength.

Optics EXPRESS

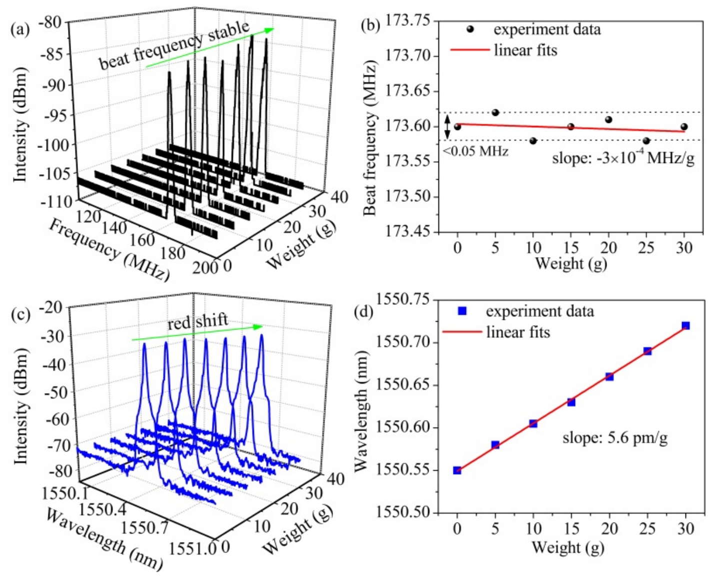

Fig. 5. Beat frequency and lasing wavelength of the DFB fiber laser under various axial strains; Beat signals (a) and optical spectra (c) of the DFB fiber laser under different weights, and Beat frequency (b) and lasing wavelength (d) of the DFB fiber laser as a function of hung weights.

We investigated the beat frequency evolutions of side-polished DFB fiber lasers created with different polishing roughness. The roughness of the polished surfaces is directly related to the grain size of the abrasive papers. Using abrasive papers with larger mesh (i.e. smaller grain size) generally leads to smoother surfaces on fiber (i.e. lower roughness). Three DFB fiber lasers were side-polished in the same direction (i.e. at an angle θ = + 45° with the original slow axis) using 7000, 5000, and 3000 mesh abrasive papers (i.e. grain sizes of 1.8, 2.6, and 5.0 μm), respectively. The pump power was fixed to 130 mW in this experiment. Figures 6(a1), 6(a2), and 6(a3) provide the microscope images of the side-polished surfaces of EDFs with various polishing roughness. According to [32], the coarse abrasive induces numerous fractures, scratches, and waviness along the fiber axis, and it could produce a brittle surface with high amplitude of surface fluctuation. In contrast, the fine abrasive tends to produce a smooth surface with little debris and minor pitting. As a result, different polishing roughness will introduce different residual stress in the fiber, leading to a different refractive index change and/or birefringence variation. As shown in Figs. 6(b1)-6(b3), the polishing roughness has a significant effect on the beat frequency shift and the birefringence variation. For the three side-polished DFB fiber lasers fabricated by 7000, 5000, and 3000 mesh abrasive papers, their beat frequencies drift to higher values with increasing polished thickness, including a transition from the initial 173.6 MHz to 1010.8 MHz (Fig. 6(b1)), 146.4 MHz to 1508.5 MHz (Fig. 6(b2)), and 133.8 MHz to 1601.2 MHz (Fig. 6(b3)) at a terminated polished thickness of 1.3, 0.7, and 0.7 μm, respectively. These beat frequency shifts correspond to birefringence changes of 6.3×10^{-6}, 1.0×10^{-5}, and 1.1×10^{-5}, respectively. Moreover, the SNRs of the beat signals gradually decrease during the polishing process. The evolutions of the beat frequency and SNR with increasing polished thickness are extracted from Figs. 6(b1)-6(b3) and then demonstrated in Figs. 6(c1)-6(c3), respectively. For these three side-polished DFB fiber lasers created by 7000, 5000, and 3000 mesh abrasive papers, their beat frequencies shift toward higher frequencies with increasing polished thickness at a slope of 272.59, 361.51, and 165.82 MHz/μm, and their SNRs decrease with increasing polished thickness at a slope of –4.51, –14.14, and –26.61 dB/μm, respectively. It is evident that the abrasive paper with a low roughness will be beneficial for fine-tuning the beat frequency. On the contrary, the abrasive paper with a high roughness can remove the beat signal quickly, and hence provides a new method for creating single polarization DFB fiber lasers.

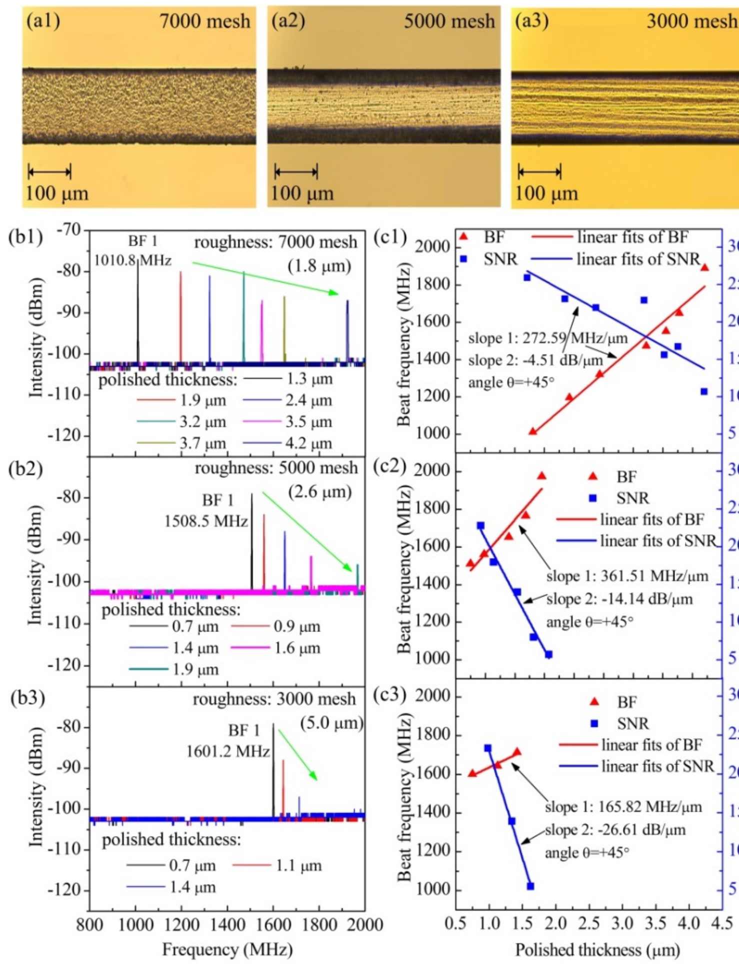

Fig. 6. Beat frequency (BF) evolutions of the side-polished DFB fiber laser using abrasive papers of varying roughness. (a1), (a2), and (a3) Microscope images of the side-polished surfaces of EDFs with various roughness of 7000, 5000, and 3000 mesh; (b1), (b2), and (b3) Beat frequency evolutions with increasing polished thickness; (c1), (c2), and (c3) Beat frequency and SNR as a function of polished thickness.

Subsequently, we investigated the beat frequency evolutions of DFB fiber lasers polished in different directions. Nine similar DFB fiber laser samples (i.e. s1 - s9 in Fig. 7) were side polished using the same 7000 mesh abrasive paper in three different directions (i.e. at an angle $\theta = 0°$, + 90°, and + 45° with the original slow axis). It should be noted that the angle θ with the original slow axis was found out in advance from the transverse-load response of the DFB fiber laser [30]. As shown in Fig. 7, the beat frequencies of all these DFB fiber lasers polished in different directions drift to higher values with increasing polished thickness, which is different from the phenomenon reported in [16], i.e., the beat frequencies shifted to higher values when the fiber laser was exposed to UV beam along the slow axis, whereas the beat frequencies shifted to lower values when the fiber laser was exposed along the fast axis. Figure 7 shows that the beat frequency shift at $\theta = +45°$ (i.e. in the direction between the original slow axis and fast axis) is noticeably smaller than those at $\theta = 0°$ and at $\theta = +90°$

Optics EXPRESS

with the same polished thickness. The orientation dependence shown in this experiment may result from the interactions between the polishing-induced asymmetry in internal stress distribution with the original fiber birefringence.

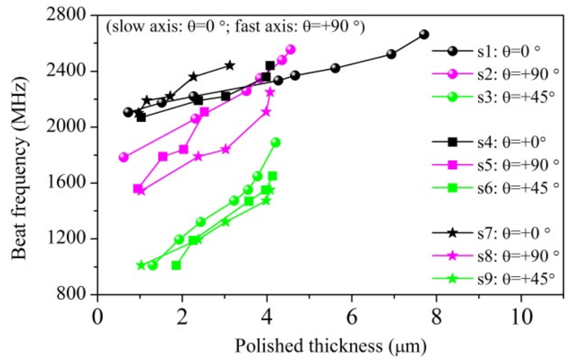

Fig. 7. Beat frequencies of DFB fiber lasers side polished in different directions (i.e. $\theta = 0°$, + 90°, and + 45°) as a function of polished thickness.

A two-dimensional side polishing was also studied for fine-tuning the beat frequency of a DFB fiber laser. At first, the DFB fiber laser was side polished using a 7000 mesh abrasive paper in the selected direction (i.e. at an angle $\theta = + 45°$ with the original slow axis). During the first side polishing process, as shown in the yellow area in Fig. 8(a) and red line in Fig. 8(b), the beat frequency shifts rapidly from the initial 181.4 MHz (O_0) to 1060.8 MHz (O_1) with a primary polished thickness of 1.4 μm, and further shifts toward higher frequencies to 2080.4 MHz (O_2) with a slope of 352.59 MHz/μm when the DFB fiber laser was polished by a thickness of 4.3 μm. The birefringence change corresponding to the beat frequency shift from O_0 to O_2 is 1.4×10^{-5}.

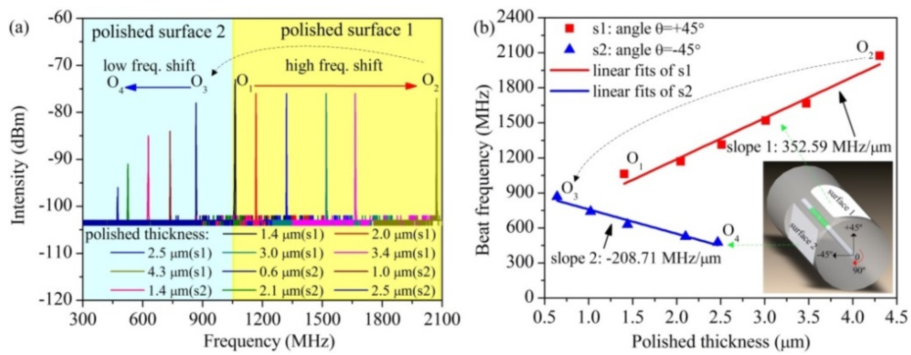

Fig. 8. (a) Beat frequency evolutions during a two-dimensional side polishing process; (b) Beat frequency as a function of polished thickness (inset: the schematic of a two-dimensional side-polished DFB fiber laser, surface1 and 2 represent the orthogonal first and secondary side-polished fiber surfaces, respectively).

Subsequently, a secondary fiber side polishing process was carried out on the side-polished DFB fiber laser in the direction (i.e. at an angle $\theta = -45°$) perpendicular to the first polishing direction (i.e. at an angle $\theta = + 45°$), as illustrated in the insert of Fig. 8(b). During the secondary side polishing process, as shown in the green area in Fig. 8(a) and blue line in Fig. 8(b), the beat frequency shifts rapidly from the initial 2080.4 MHz (O_2) to 870.5 MHz (O_3) with a primary polished thickness of 0.6 μm, and further shifts toward lower frequencies with a slope of −208.71 MHz/μm to 475.5 MHz (O_4) with a polished thickness of 2.5 μm. The birefringence change corresponding to the beat frequency shift from O_2 to O_4 is −1.2 ×

10^{-5}. Figure 8(b) demonstrates that the beat frequency of DFB fiber laser has been tuned in a wide frequency range from 475.5 MHz to 2080.4 MHz. These results illustrate that the birefringence change induced by side polishing is closely related to the polishing directions. The first side polishing will increase the asymmetry in fiber geometry and stress distribution, leading to an increased fiber birefringence. In contrast, the secondary side polishing in the orthogonal direction will reduce the asymmetry in fiber geometry and stress distribution, and hence leads to a decreased fiber birefringence. Moreover, it should be noted that an expanded frequency tuning range and a more precise frequency tuning could be achieved using the two-dimensional side polishing method rather than using the primitive one-side polishing method. As a result, the two-dimensional side polishing method could further be developed for use in multiplexing a large number of fiber laser sensors using the FDM technique.

Furthermore, we also demonstrated the possibility of the fiber side polishing method used for realizing a single-polarization DFB fiber laser. At first, as shown in Figs. 9(a1) and 9(b1), a dual-polarization DFB fiber laser generated a beat frequency of 137.4 MHz at a pump power of 80 mW. And then, the dual-polarization DFB fiber laser was side polished by a 7000 mesh abrasive paper. The beat frequency shifted towards higher frequencies with a decreasing beat signal SNR during this process. The evolutions of the beat frequency and the beat signal SNR are similar to those demonstrated in Figs. 6(b1) and 6(c1). In case the DFB fiber laser was polished by a thickness of 4.2 μm, the beat signal disappeared while the laser signal remained in the optical spectrum with an adequate SNR of 45.1 dB, as shown in Figs. 9(a2) and 9(b2), which means that the DFB fiber laser side polished with a thickness of 4.2 μm operates in a single polarization at the pump power of 80 mW. Subsequently, we increase the pump power to 90 mW. The beat signal appeared again at the beat frequency of 2113.8 MHz with a low SNR of 15.9 dB, and the SNR in the optical spectrum also increased slightly from 45.1 dB to 46.6 dB, as shown in Figs. 9(a3) and 9(b3). These results indicate that side polishing on DFB fiber lasers by a certain thickness will significantly raise the threshold pump power for one polarization mode, and hence could be used for fabricating novel single-polarization DFB fiber lasers.

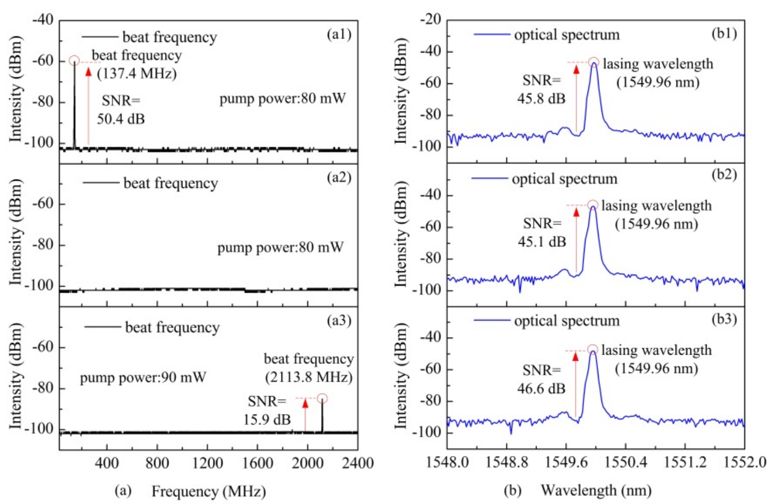

Fig. 9. Side polishing used for realizing a single-polarization DFB fiber laser. (a) Beat signals of the DFB fiber laser; (b) Optical spectra of the DFB fiber laser. (a1 and b1 correspond to the original dual-polarization DFB fiber laser at a pump power of 80 mW; a2 and b2 correspond to the single-polarization side-polished DFB fiber laser with a polished thickness of 4.2 μm at the same pump power of 80 mW; a3 and b3 correspond to the dual-polarization side-polished DFB fiber laser with a polished thickness of 4.2 μm at an increased pump power of 90 mW).

5. Conclusion

A side polishing method has been proposed and demonstrated for tuning the beat frequency of DFB fiber lasers. Beat frequency evolutions in DFB fiber lasers were studied, and the beat frequency was found to be dependent on polished thickness, roughness, and direction. Moreover, the beat frequency could be fine-tuned using the abrasive paper with a grain size of 1.8 μm (i.e. 7000 mesh). We found that the beat frequency of DFB fiber lasers shifted toward higher frequencies with increasing polished thickness, whereas the beat frequency shifted toward lower frequencies using a secondary side polishing process in the direction orthogonal to the first polished surface. Hence, the beat frequency of DFB fiber lasers has been tuned in a wide frequency range from 475.5 MHz to 2080.4 MHz, corresponding to the birefringence varying from 3.5×10^{-6} to 1.6×10^{-5}. As a result, the side polishing method can be developed for frequency division multiplexing for heterodyning fiber laser sensors or realizing novel single-polarization DFB fiber lasers.

Funding

National Natural Science Foundation of China (grant nos. 61875128, 61505120, 61425007 and 61635007), Guangdong Natural Science Foundation (grant nos. 2017A010102015, 2015B010105007 and 2014A030308007), Science and Technology Innovation Commission of Shenzhen (grant nos. JCYJ20170302143105991, JCYJ20170412105604705, JCYJ20160427104925452 and GRCK2017082111254221), Research Funding from Shenzhen University (grant no. 2017019), and Development and Reform Commission of Shenzhen Municipality Foundation.

References

1. Q. Li, F. Yan, W. Peng, T. Feng, S. Feng, S. Tan, P. Liu, and W. Ren, "DFB laser based on single mode large effective area heavy concentration EDF," Opt. Express **20**(21), 23684–23689 (2012).
2. J. T. Kringlebotn, J. L. Archambault, L. Reekie, and D. N. Payne, "Er^{3+}:Yb^{3+}-codoped fiber distributed-feedback laser," Opt. Lett. **19**(24), 2101–2103 (1994).
3. S. Agger, J. H. Povlsen, and P. Varming, "Single-frequency thulium-doped distributed-feedback fiber laser," Opt. Lett. **29**(13), 1503–1505 (2004).
4. J. Hubner, P. Varming, and M. Kristensen, "Five wavelength DFB fibre laser source for WDM systems," Electron. Lett. **33**(2), 139–140 (1997).
5. M. Ibsen, S. U. Alam, M. N. Zervas, and A. B. Grudinin, "8- and 16-channel all-fiber DFB laser WDM transmitters with integrated pump redundancy," IEEE Photonics Technol. Lett. **11**(9), 1114–1116 (1999).
6. H. Al-Taiy, N. Wenzel, S. Preußler, J. Klinger, and T. Schneider, "Ultra-narrow linewidth, stable and tunable laser source for optical communication systems and spectroscopy," Opt. Lett. **39**(20), 5826–5829 (2014).
7. G. A. Cranch, "Frequency noise reduction in erbium-doped fiber distributed-feedback lasers by electronic feedback," Opt. Lett. **27**(13), 1114–1116 (2002).
8. W. Zhang, Y. C. Lai, J. A. R. Williams, C. Lu, L. Zhang, and I. Bennion, "A fibre grating DFB laser for generation of optical microwave signal," Opt. Laser Technol. **32**(5), 369–371 (2000).
9. O. Hadeler, E. Rønnekleiv, M. Ibsen, and R. I. Laming, "Polarimetric distributed feedback fiber laser sensor for simultaneous strain and temperature measurements," Appl. Opt. **38**(10), 1953–1958 (1999).
10. J. T. Kringlebotn, W. H. Loh, and R. I. Laming, "Polarimetric Er^{3+}-doped fiber distributed-feedback laser sensor for differential pressure and force measurements," Opt. Lett. **21**(22), 1869–1871 (1996).
11. S. W. Løvseth, J. T. Kringlebotn, E. Rønnekleiv, and K. Bløtekjaer, "Fiber distributed-feedback lasers used as acoustic sensors in air," Appl. Opt. **38**(22), 4821–4830 (1999).
12. A. Suemasa, A. Shimo-Oku, K. I. Nakagawa, and M. Musha, "Developments of high frequency and intensity stabilized lasers for space gravitational wave detector DECIGO/B-DECIGO," Ceas Space J. **9**(4), 485–491 (2017).
13. H. Renner, "Effective-index increase, form birefringence and transition losses in UV-side-illuminated photosensitive fibers," Opt. Express **9**(11), 546–560 (2001).
14. A. M. Vengsarkar, Q. Zhong, D. Inniss, W. A. Reed, P. J. Lemaire, and S. G. Kosinski, "Birefringence reduction in side-written photoinduced fiber devices by a dual-exposure method," Opt. Lett. **19**(16), 1260–1262 (1994).
15. T. Guo, A. C. Wong, W. S. Liu, B. O. Guan, C. Lu, and H. Y. Tam, "Beat-frequency adjustable Er^{3+}-doped DBR fiber laser for ultrasound detection," Opt. Express **19**(3), 2485–2492 (2011).
16. Y. Zhang, Y. N. Tan, T. Guo, and B. O. Guan, "Beat frequency trimming of dual-polarization fiber grating lasers for multiplexed sensor applications," Opt. Express **19**(1), 218–223 (2011).

Optics EXPRESS

17. S. A. Babin, D. V. Churkin, A. E. Ismagulov, S. I. Kablukov, and M. A. Nikulin, “Single frequency single polarization DFB fiber laser,” Laser Phys. Lett. **4**(6), 428–432 (2007).
18. J. L. Philipsen, M. O. Berendt, P. Varming, V. C. Lauridsen, J. H. Povlsen, J. Hubner, M. Kristensen, and B. Palsdottir, “Polarisation control of DFB fibre laser using UV-induced birefringent phase-shift,” Electron. Lett. **34**(7), 678–679 (1998).
19. L. Jin, Y. Liang, M. P. Li, L. Cheng, J. Li, and B. O. Guan, “A 16-element multiplexed heterodyning fiber grating laser sensor array,” J. Lightwave Technol. **32**(22), 4410–4415 (2014).
20. J. He, Y. Wang, C. Liao, Q. Wang, K. Yang, B. Sun, G. Yin, S. Liu, J. Zhou, and J. Zhao, “Highly birefringent phase-shifted fiber Bragg gratings inscribed with femtosecond laser,” Opt. Lett. **40**(9), 2008–2011 (2015).
21. W. Fan, B. Chen, X. Li, L. Chen, and Z. Lin, “Stress-induced single polarization DFB fiber lasers,” Opt. Commun. **204**(1), 157–161 (2002).
22. R. Ulrich, S. C. Rashleigh, and W. Eickhoff, “Bending-induced birefringence in single-mode fibers,” Opt. Lett. **5**(6), 273–275 (1980).
23. Z. E. Harutjunian, W. H. Loh, R. I. Laming, and D. N. Payne, “Single polarisation twisted distributed feedback fibre laser,” Electron. Lett. **32**(4), 346 (1996).
24. M. N. Zervas, R. Wilmshurst, and L. M. Walker, “Twisted hi-bi fiber distributed-feedback lasers with controllable output state of polarization,” Opt. Lett. **38**(9), 1533–1535 (2013).
25. R. H. Stolen, “Polishing-induced birefringence in single-mode fibers,” Appl. Opt. **25**(3), 344–347 (1986).
26. J. Zhao, G. Yin, C. Liao, S. Liu, J. He, B. Sun, G. Wang, X. Xu, and Y. Wang, “Rough side-polished fiber with surface scratches for sensing applications,” IEEE Photonics J. **7**(3), 1–7 (2015).
27. J. Zhao, S. Cao, C. Liao, Y. Wang, G. Wang, X. Xu, C. Fu, G. Xu, J. Lian, and Y. Wang, “Surface plasmon resonance refractive sensor based on silver-coated side-polished fiber,” Sens. Actuators B Chem. **230**, 206–211 (2016).
28. B. O. Guan, L. Jin, Y. Zhang, and H. Y. Tam, “Polarimetric heterodyning fiber grating laser sensors,” J. Lightwave Technol. **30**(8), 1097–1112 (2012).
29. T. Erdogan and V. Mizrahi, “Characterization of UV-induced birefringence in photosensitive Ge-doped silica optical fibers,” J. Opt. Soc. Am. B **11**(10), 2100–2105 (1994).
30. Y. Zhang, B. O. Guan, and H. Y. Tam, “Characteristics of the distributed Bragg reflector fiber laser sensor for lateral force measurement,” Opt. Commun. **281**(18), 4619–4622 (2008).
31. J. Zhou, K. Guo, J. He, M. Hou, Z. Zhang, C. Liao, Y. Wang, G. Xu, and Y. Wang, “Novel fabrication technique for phase-shifted fiber Bragg gratings using a variable-velocity scanning beam and a shielded phase mask,” Opt. Express **26**(10), 13311–13321 (2018).
32. M. Li, Z. Bai, F. Zhang, M. Hou, Y. Wang, C. Liao, W. Jin, and Y. Wang, “Red shift of side-polished fiber surface plasmon resonance sensors with silver coating and inhibition by gold plating,” IEEE Photonics J. **9**(3), 1–13 (2017).